

# State of the art of electron spectrometers at the ALS

Alexei Fedorov \$\$

/November 13 2001, ALS monthly meeting/

---

\$\$ *Supported by:*



Plan:

Orientation

Photoelectron Spectroscopy

Instrumentation

Gammadata-Scienta spectrometers

Examples of the research

# Scientia spectrometers at ALS

**GAMMADATA  
—SCIENTIA—**

**ELECTRON SPECTROMETER  
SCIENTIA SES 2002**

**Features:**

- < 2 meV energy resolution
- Angle multiplexing record from large area samples
- Extremely low noise, high stability power supplies
- Double  $\mu$ -metal shielding
- 2-D CCD multi-channel detection system, > 400 energy channels
- Light weight design

**Main application:**

- High resolution electron spectroscopy
- High resolution photoelectron diffraction
- High resolution angular resolved spectroscopy
- High resolution spectromicroscopy



The SES 2002 is a full hemispherical detector system consisting of a detector system connected to a specially designed electronics and data acquisition system. The detector system is a micro-high resolution spectroscopy system with a photoelectron detector and a photoelectron detector. The detector is equipped with an acceptance angle of 45 mm to allow for a wide range of experiments. Switching between different modes is done by a detector enables ing/retarding multi-element detection.

In the unique angular mode a high-voltage system is made to coincide with a highly stable adjustment facility to achieve a slit plane parallel to the sample. The high voltage focusing, ensuring close to the multi angle recording. The system is designed to decouple energy resolution down to acceptance angle reducing the need for a computer via a fib lowest pass energies. Double  $\mu$ -metal shielding ensures optimum performance is achieved with minimal loss even in the presence of stray magnetic fields.

Gammadata Scientia AB  
P.O. Box 15 120 | S-750 15 Uppsala | Sweden  
Phone: +46 18 480 58 00 | Fax: +46 18 555 888 | E-mail: info@gammadata.se | Internet: www.gammadata.se

**GAMMADATA  
—SCIENTIA—**

**ELECTRON SPECTROMETER  
SCIENTIA SES 10**

**Features:**

- < 3 meV energy resolution
- Angle multiplexing record with variable angular dispersion and resolution
- Extremely low noise, high stability power supplies
- Double  $\mu$ -metal shielding
- 2-D multi-channel detection system, > 400 energy channels

**Main application:**

- High resolution electron spectroscopy
- High resolution photoelectron diffraction
- High resolution angular resolved spectroscopy



The SES 100 is a new, high performance angular resolution can be achieved. The interface is available to the user to write the same technology. It is a small loss of count rate enables the user to write the same technology. The SES 100 is a new, high performance angular resolution can be achieved. The interface is available to the user to write the same technology. The SES 100 is a new, high performance angular resolution can be achieved. The interface is available to the user to write the same technology.

The SES 100 has double  $\mu$ -metal shielding and utilizes the high voltage system to assist the user to work with a variable angular power supplies needed for large sample analysis. The unique angular mode allows for a wide range of experiments. The system is designed to decouple energy resolution down to acceptance angle reducing the need for a computer via a fib lowest pass energies. Double  $\mu$ -metal shielding ensures optimum performance is achieved with minimal loss even in the presence of stray magnetic fields.

Gammadata Scientia AB  
P.O. Box 15 120 | S-750 15 Uppsala | Sweden  
Phone: +46 18 480 58 00 | Fax: +46 18 555 888 | E-mail: info@gammadata.se | Internet: www.gammadata.se

**GAMMADATA  
—SCIENTIA—**

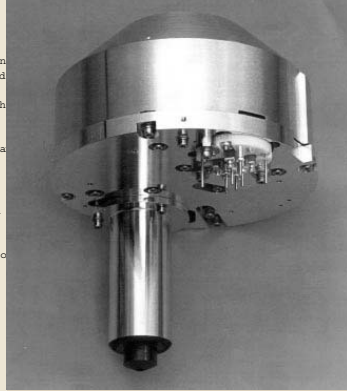
**ELECTRON SPECTROMETER  
SCIENTIA SES 50**

**Features:**

- < 3 meV energy resolution
- Angle multiplexing record from small area samples
- Extremely low noise, high stability power supplies
- Customized lens design
- Multi-channel resistive array detector

**Main application:**

- High resolution electron spectroscopy
- High resolution photo-electron diffraction
- High resolution angular resolved spectroscopy



The SES 50 is a very high resolution detector system consisting of a detector system connected to a specially designed electronics and data acquisition system. The detector system is a micro-high resolution spectroscopy system with a photoelectron detector and a photoelectron detector. The detector is equipped with an acceptance angle of 45 mm to allow for a wide range of experiments. Switching between different modes is done by a detector enables ing/retarding multi-element detection.

The multi-element lens system is designed to assist the user to work with a variable angular power supplies needed for large sample analysis. The unique angular mode allows for a wide range of experiments. The system is designed to decouple energy resolution down to acceptance angle reducing the need for a computer via a fib lowest pass energies. Double  $\mu$ -metal shielding ensures optimum performance is achieved with minimal loss even in the presence of stray magnetic fields.

Gammadata Scientia AB  
P.O. Box 15 120 | S-750 15 Uppsala | Sweden  
Phone: +46 18 480 58 00 | Fax: +46 18 555 888 | E-mail: info@gammadata.se | Internet: www.gammadata.se

BL-10.0.1 (2)

BL-12.0.1 (1)

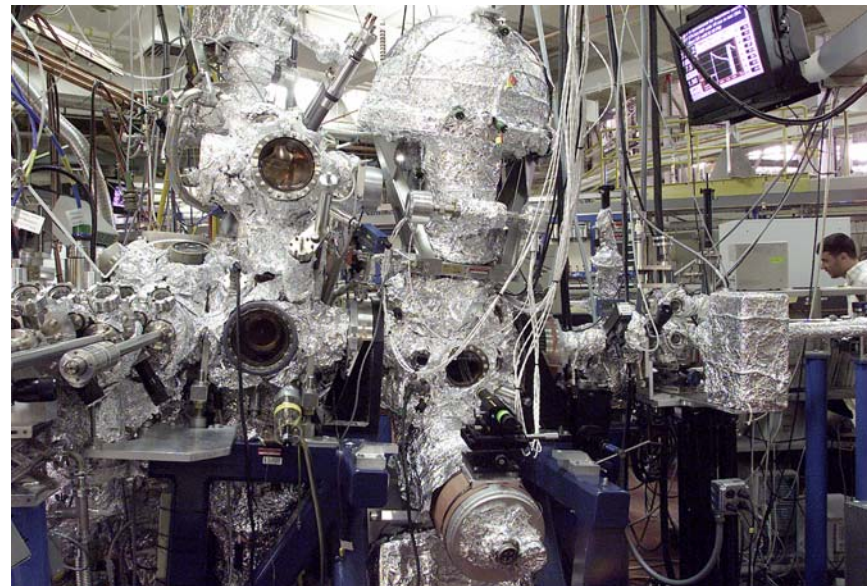
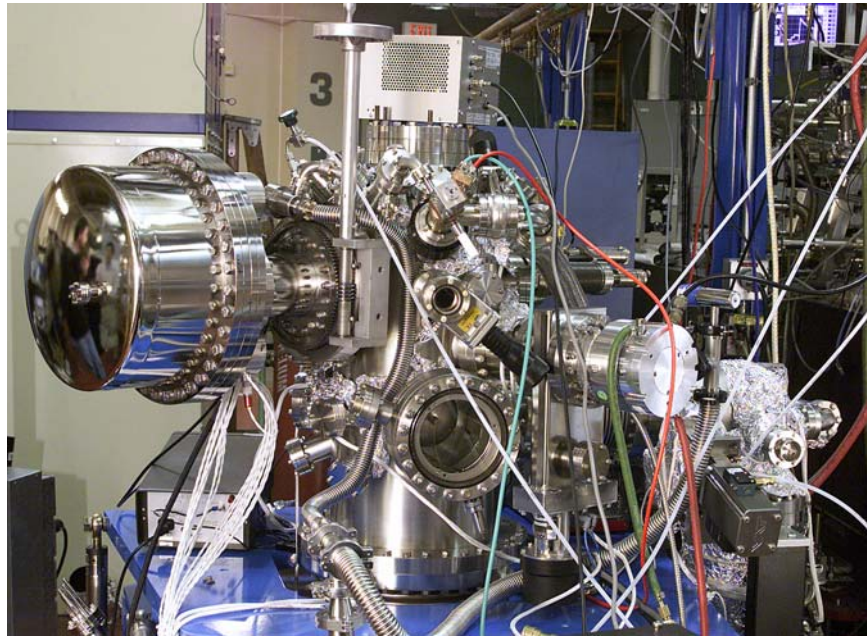
BL-7.0.1

BL-12.0.1

BL-9.3.2

BL-8.0.1

NONE



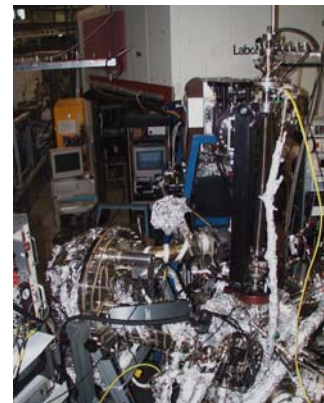
Other facilities also have it:

NSLS, Brookhaven: SES-200 (1)

SSRL, Stanford: SES-200 (1+)

SRC, Stoughton: SES-200 (1+), SES-50

CAMD, Baton Rouge: SES-200 (1)



# Photoemission /inverse photoemission/

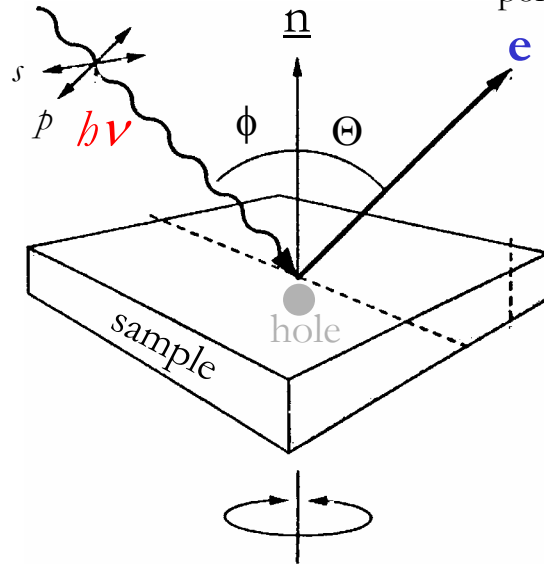
## Experiment

### Excitation Radiation

- photon energy
- polarization
- angle of incidence

### Photoelectrons

- kinetic energy
- emission angle
- polarization



### Important parameters:

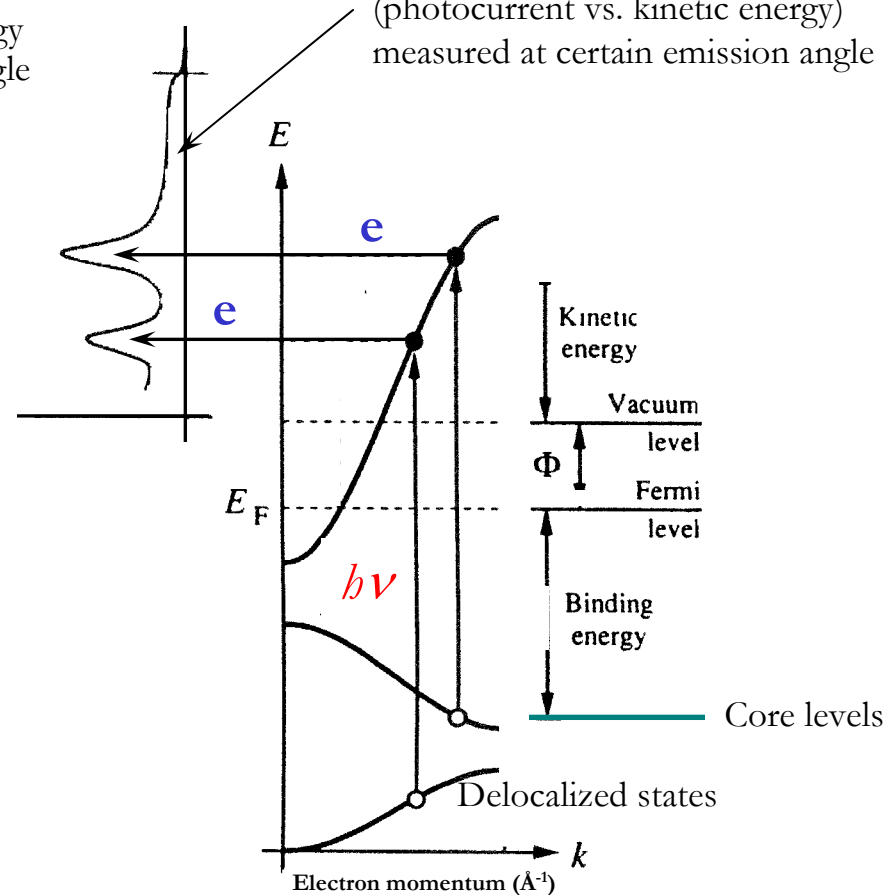
Energy resolution ( $\sim 20$  meV)

Angular resolution ( $\sim 2^\circ$ )

## Data

### Energy Distribution Curves

(photocurrent vs. kinetic energy)  
measured at certain emission angle



Aim: learn Electronic structure or Chemical composition

Approach: fitting Data using appropriate models



# Surface core level shifts in 4-f metals

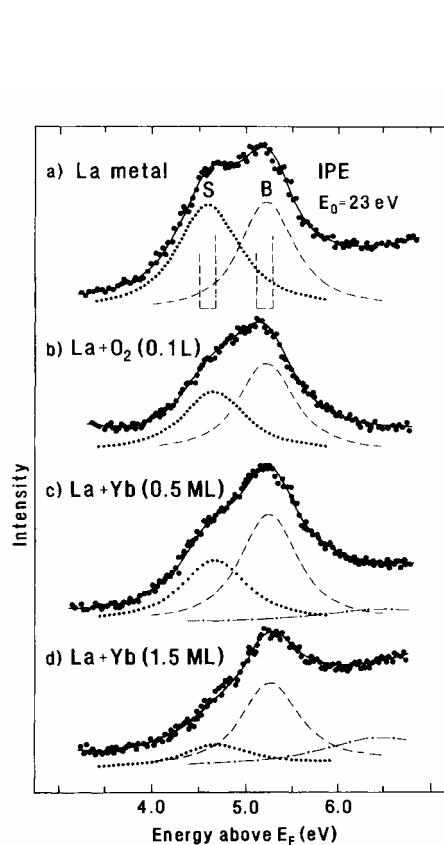


FIG. 2. Inverse photoemission spectra in the region of the  $4f^1$  electron-addition state, taken at a primary electron energy of  $E_0 = 23$  eV: (a) a clean surface of La metal; (b) after exposure to 0.1 L of oxygen; after coverage by (c) 0.5 monolayer (ML) of Yb and (d) 1.5 ML of Yb. The solid curves through the data points are the results of least-squares fits; for details see text.

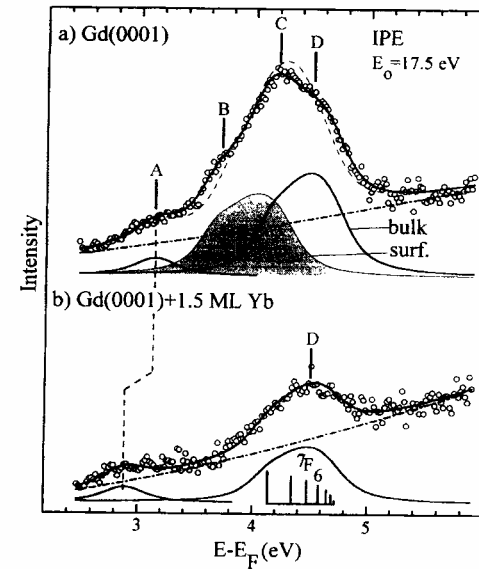
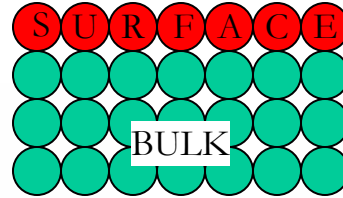


FIG. 1. IPE spectra of Gd(0001) in the region of the  $4f^8$  electron-addition state, taken at a primary electron energy of  $E_0 = 17.5$  eV: (a) clean Gd(0001) surface; (b) after coverage by 1.5 ML of Yb metal. Spectral features B, C, and D of clean Gd(0001) originate from  $4f^8$  electron-addition states in the topmost surface layer (shaded) and in the bulk (solid curve); the vertical-bar diagram in (b) gives the energies and relative intensities of the individual  $7F_J$  bulk multiplet components. The solid curves through the data points in (a) and (b) represent the results of the best least-squares fits. The dashed curve in (a) was obtained in a fit where  $\delta_s^{ea} = \delta_s^{cr}$  was assumed. For details see text.

# Electronic structure of High Temperature Superconductor And Ferromagnetic Gd

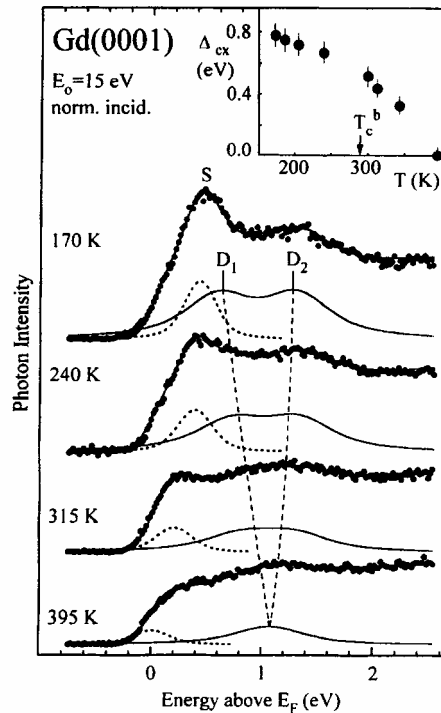


FIG. 4. Least-squares-fit analysis of selected inverse-photoemission spectra of Gd(0001) from Fig. 1 (for details, see text). The inset gives the exchange splitting  $\Delta_{ex}$  as a function of temperature.

*A.V. Fedorov et al., PRB 50, 2739 (1994)*

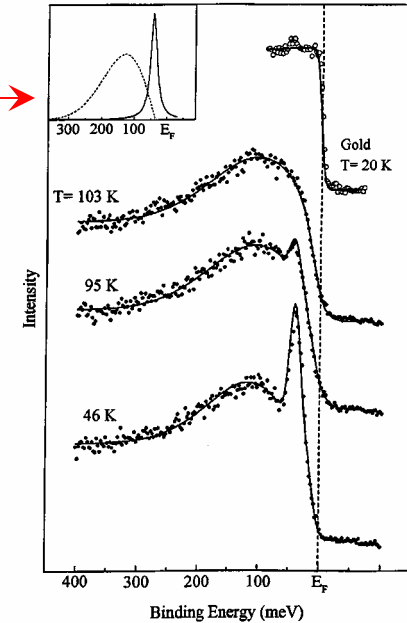


FIG. 2. Sample spectra at different temperatures showing the fit obtained using the two functions and background described in the text. The inset shows the separation of the leading edge of the broad peak from  $E_F$ , the Fermi level. The upper spectrum represents the Fermi edge obtained from an evaporated gold film.

VOLUME 82, NUMBER 10

PHYSICAL REVIEW LETTERS

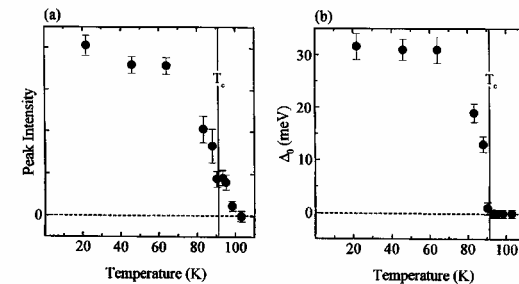
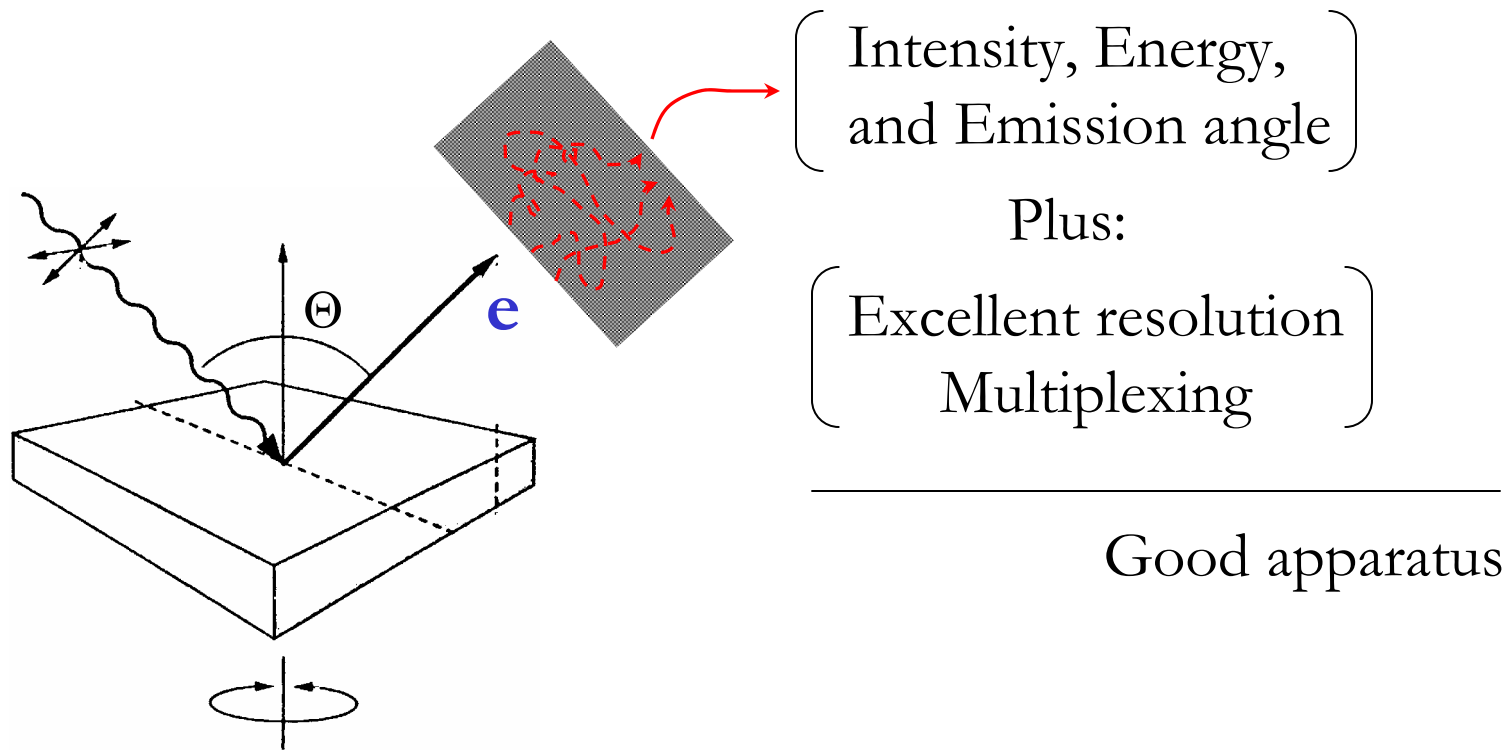


FIG. 3. (a) Intensity of the sharp peak as a function of the sample temperature. The transition temperature  $T_c$  is indicated. (b) The gap,  $\Delta_0$ , between the leading edge of the broad peak and the Fermi level as obtained from the fitting procedure.

*A.V. Fedorov et al., PRL 82, 2179 (1999)*



What is an electron spectrometer?



# Hyperbolic field analyzer

/ *M. Jacka et al., RSI 70, 2282 (1999)* /

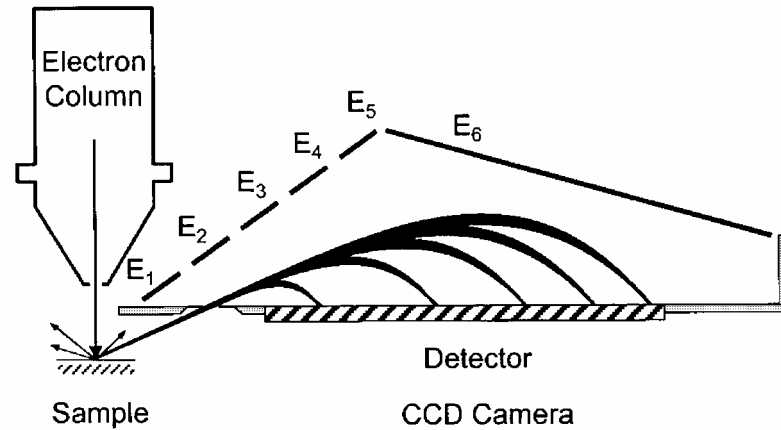


FIG. 5. The prototype HFA and electron gun, showing some electron trajectories with differing energy. The field is constructed by applying the appropriate voltages to electrodes  $E_1-E_6$ .

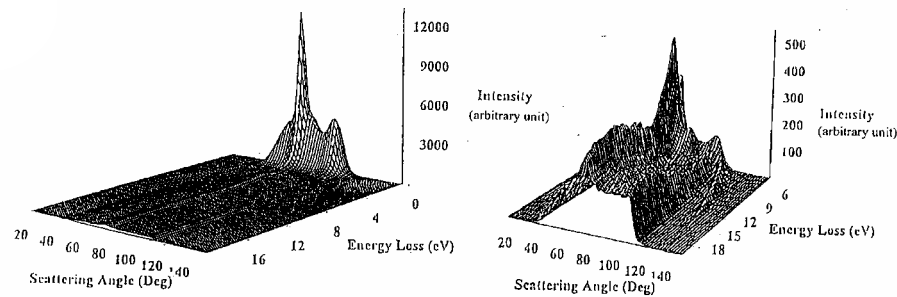


FIG. 10. 3D view of energy loss spectrum in  $e^+$ -HOPG collisions at electron incident energy of 50 eV, the left figure shows the whole spectrum and only inelastic features are shown in the right one.

# Display Analyzer

/single energy, all angles/

2640

Rev. Sci. Instrum., Vol. 72, No. 6, June 2001

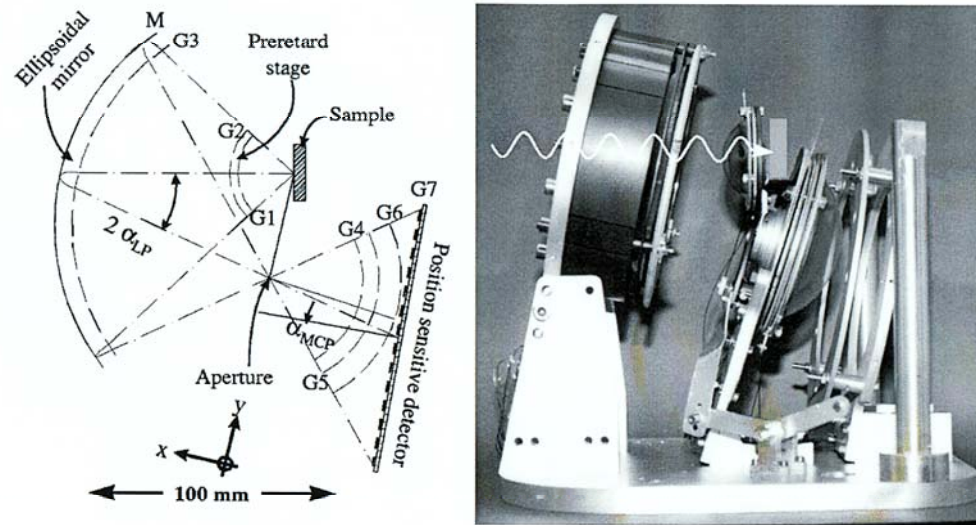


FIG. 1. Sketch showing the operation principal of the ellipsoidal display analyzer (left) with its main components, the preretardation stage, the ellipsoidal low-pass mirror, the aperture, the high-pass filter, and the detector. A photograph of the analyzer (side view) with the shielding removed is shown on the right. The light (wavy line) enters the analyzer in the horizontal plane ( $56^\circ$  relative to the sample normal).

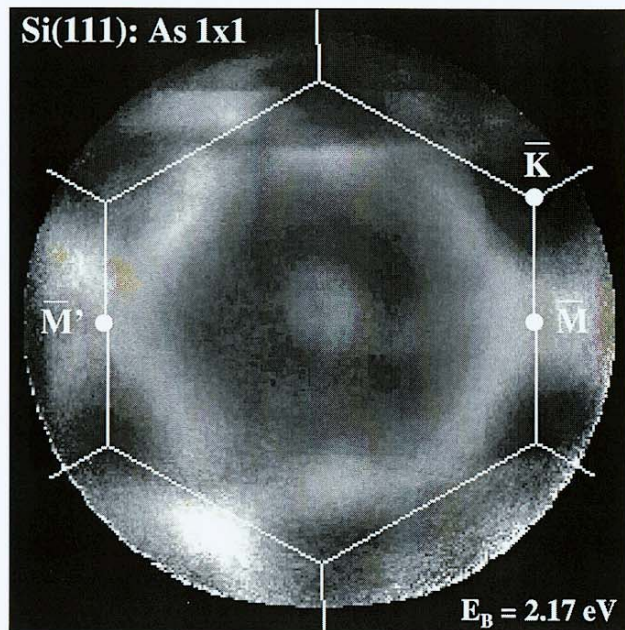


FIG. 7. Photoelectron intensity vs parallel wave vector  $I(k_{\parallel})$  at  $E_B = 2.17 \text{ eV}$  binding energy for the arsenic-terminated Si(111) surface. The surface Brillouin zone with the high-symmetry points is shown by a white line. At this binding energy the emission is dominated by the lone-pair arsenic surface state showing almost hexagonal symmetry. Total acquisition time is 100 s.

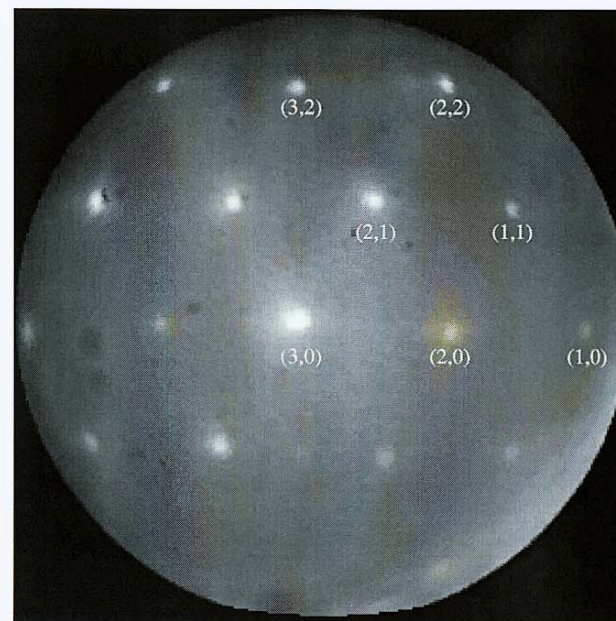


FIG. 8. LEED image of Si(111):As  $1 \times 1$  taken with the ellipsoidal display analyzer at a kinetic electron energy of  $E = 470 \text{ eV}$  and with an aperture of  $r_A = 0.5 \text{ mm}$ . LEED images can be taken without moving the analyzer or sample. The LEED pattern is tilted relative to conventional LEEDs because of the  $56^\circ$  incidence angle of the primary electron beam. Some reflections of the  $1 \times 1$  hexagonal surface Brillouin zone are indexed for clarity.

# Double toroidal analyzer

/ *C.Miron et al., RSI 68, 3728 (1997)* /

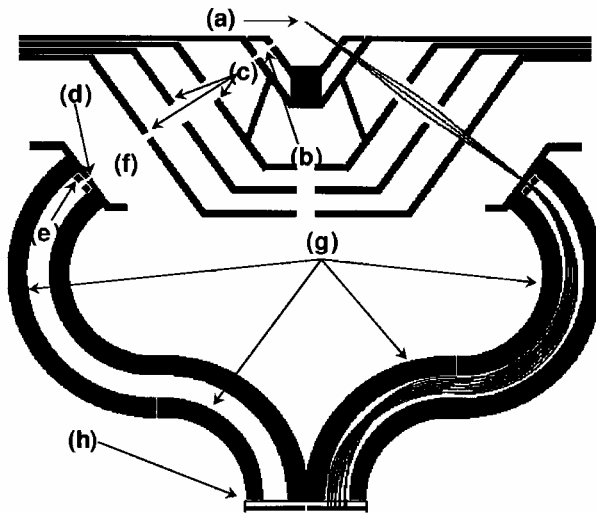


FIG. 3. Numerical simulation of electron trajectories with the DTA. The DTA main parts: (a) interaction region; (b) the two elements collimator; (c) focusing elements of the conical lens; (d) DTA input slit; (e) correction rings; (f) field-free region; (g) the four “toroidal” deflection plates; and (h) focusing region.

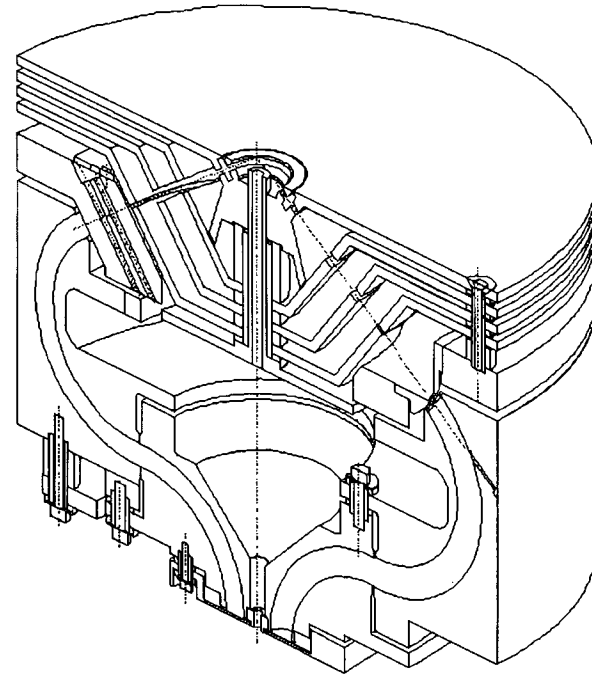


FIG. 5. Three dimensional view of the DTA's mechanical setup.

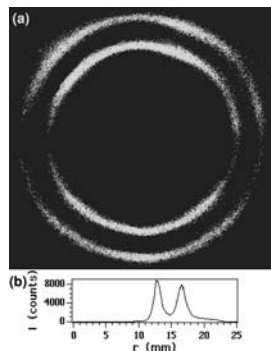


FIG. 8. a) The image on the PFD of the 1st/2nd/3rd photoionization of  $N_2O$  molecule excited with 470 eV photons, recorded with the DTA. b) The corresponding  $I(r)$  spectrum.

Energy window:  $\Delta E \sim 15\%$  PE  
Resolving power:  $E_p / \delta E \sim 100$

## Suggested reading:

- ✓ B. Wannberg, U. Gelius, and K. Sieghban, J. Phys. E, Sci. Instrum. 7, 149 (1974)
- ✓ R.C.G. Leckey, J. Electron Spectr. Relat. Phenom. 43, 183 (1987)

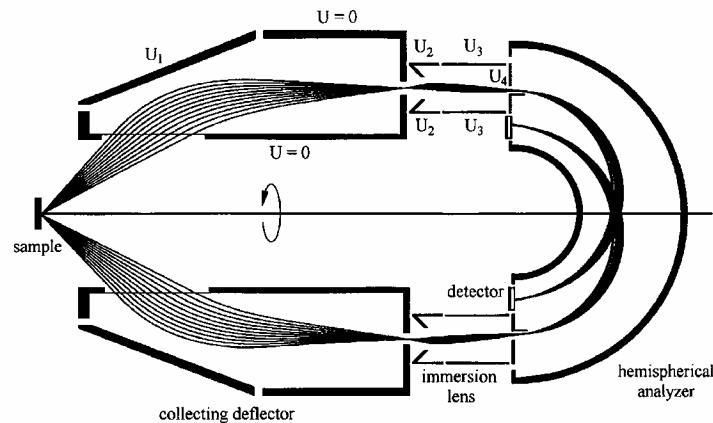
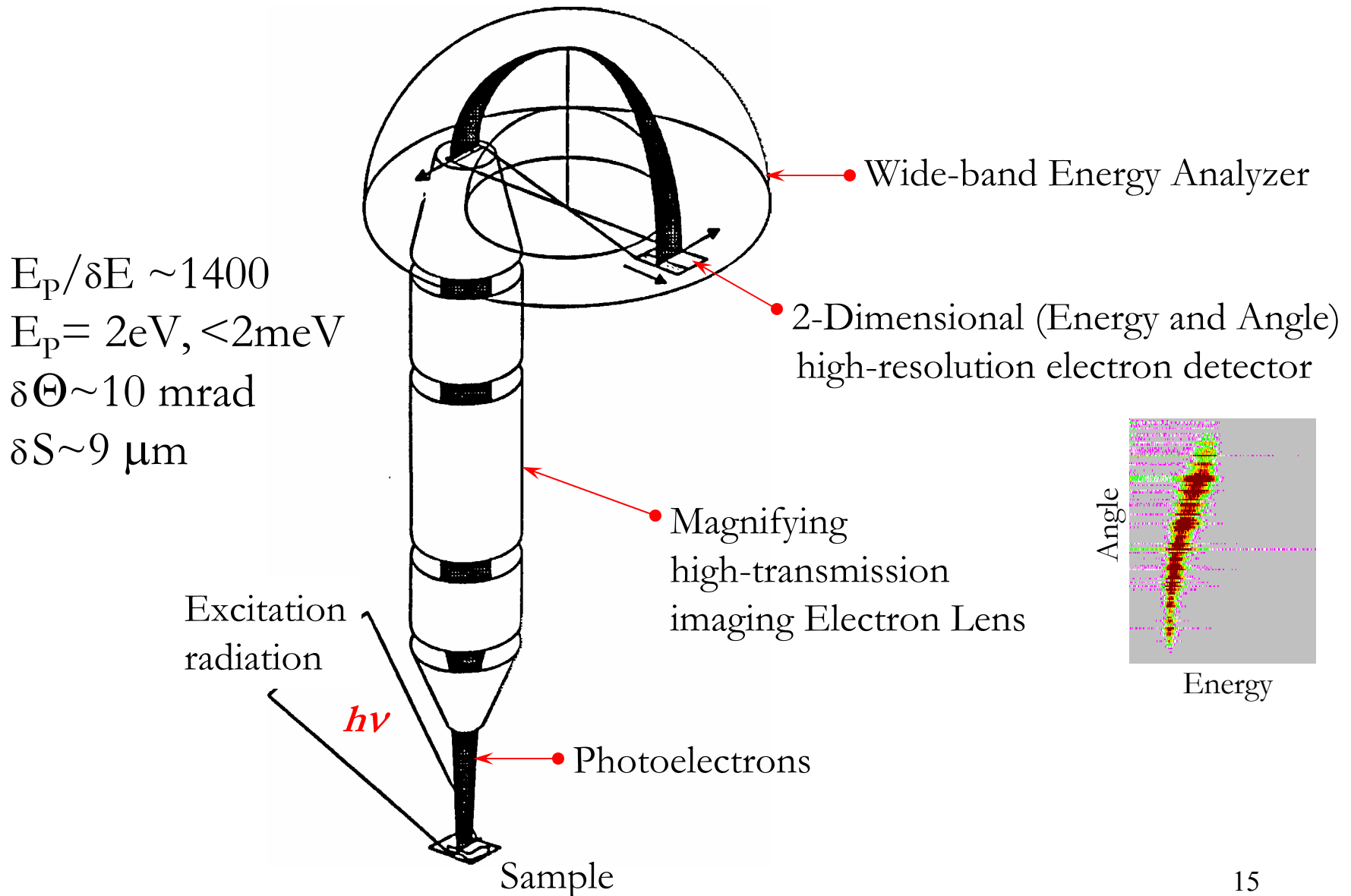


FIG. 2. A configuration of a high-transmission energy analyzer that consists of a collecting mirror of Fig. 1, a hollow coaxial cylindrical lens, and a hemispherical deflector.

*V.D. Belov and M.I. Yavor, RSI 71, 1651 (2000)*



# New Instrumentation from Gammadata-Scienta



## 2-dimensional detector

/Micro-channel plates coupled to the phosphor screen/

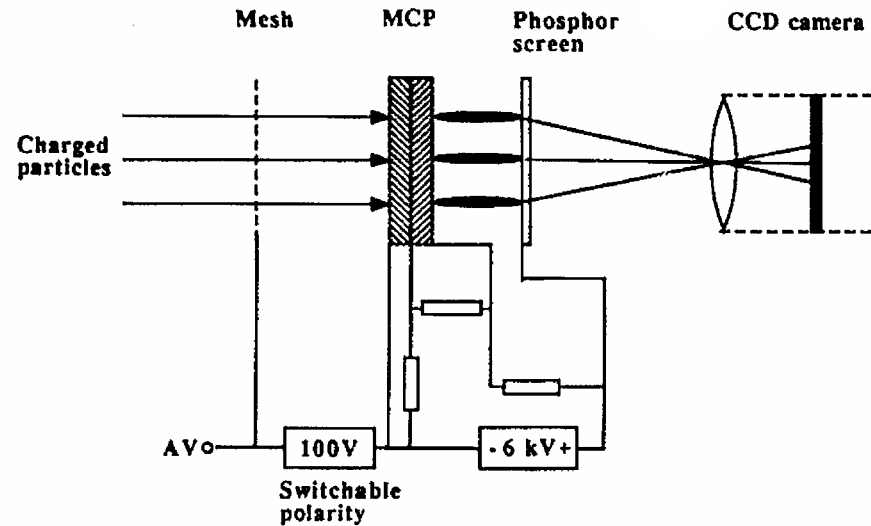
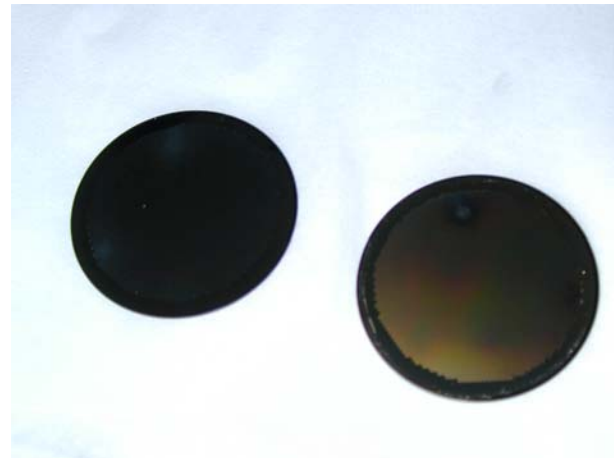
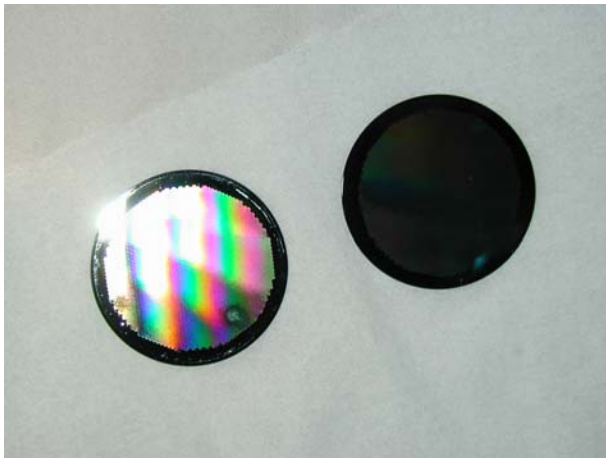
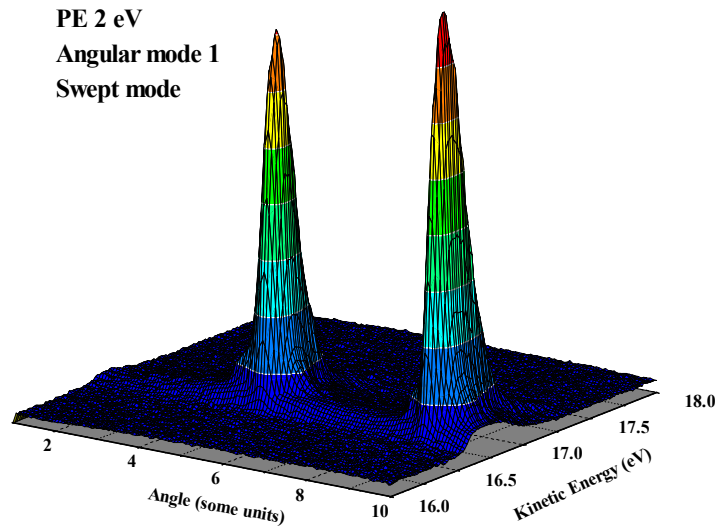
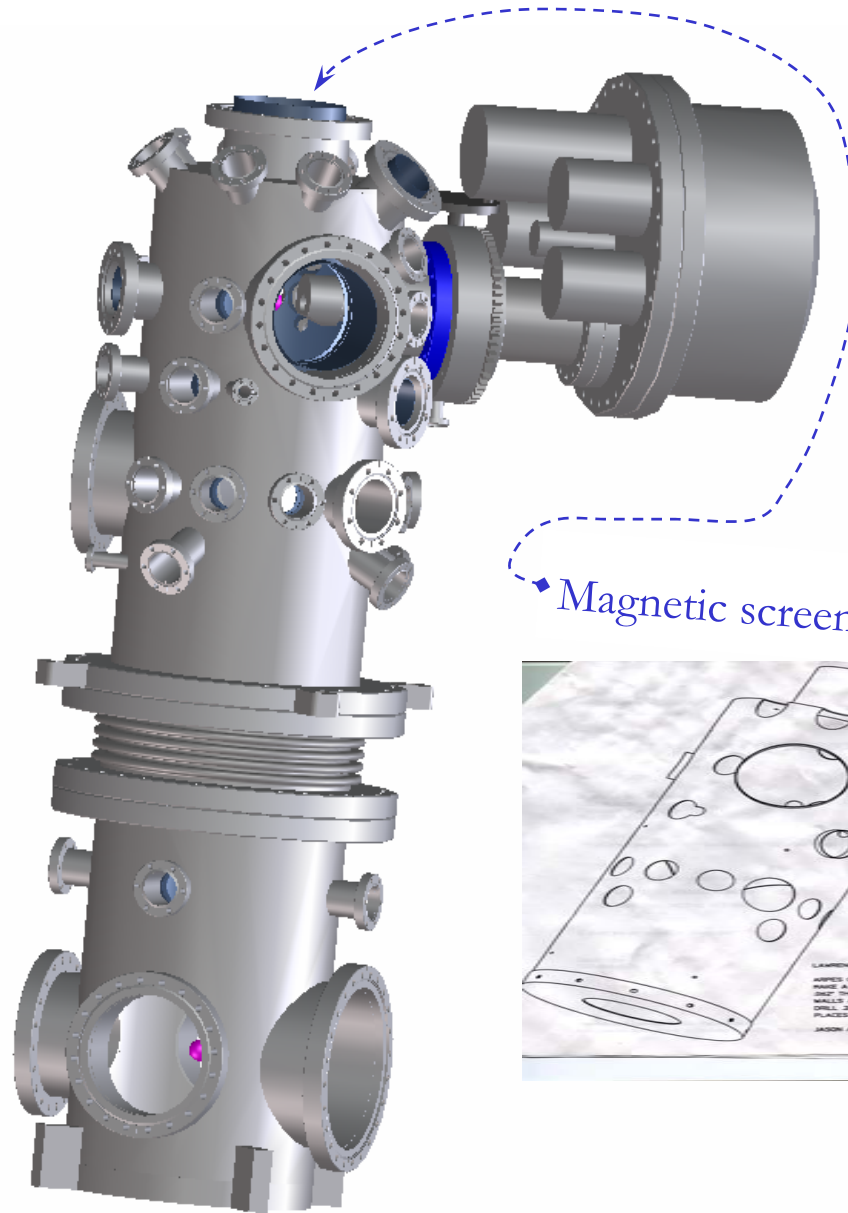


FIG. 12. Schematic drawing of the detection system.

Is it: { Fast  
Uniform  
Linear  
Stable } ?

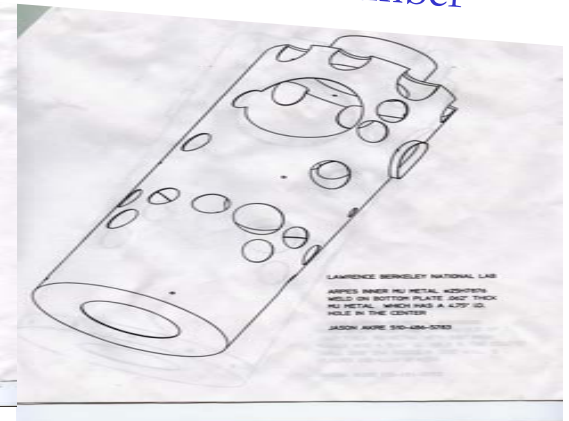
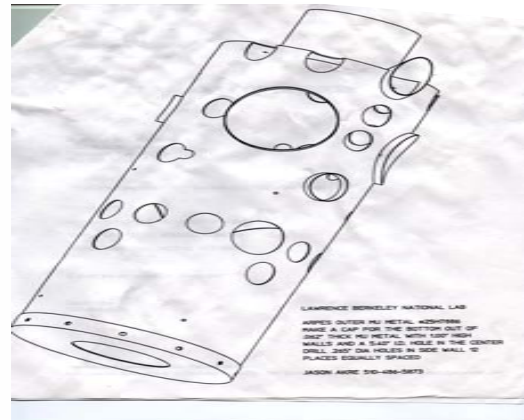
# Solving detector mysteries





Engineering expertise  
is essential for making  
our analyzers to work

Magnetic screens /  $\mu$ -metal/ go inside the chamber

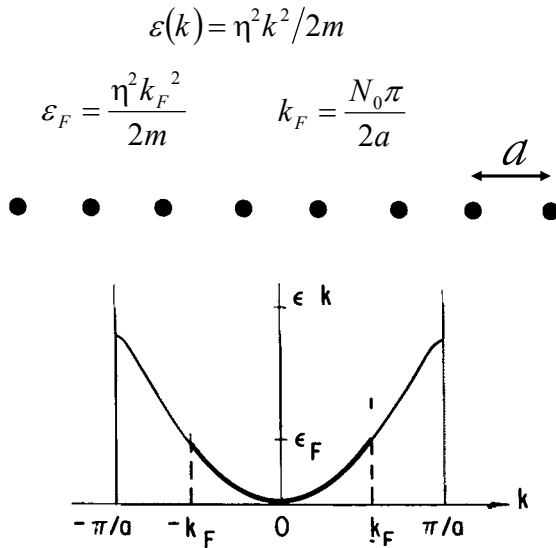


# Charge Density Waves

**R.E. Peirls**, Quantum Theory of Solids (Clarendon, Oxford, 1955); **H. Fröhlich**, Proc. R. Soc. Lond. A 223, 296 (1954);  
**A.W. Overhauser**, Phys. Rev. 167, 691 (1968); **S.-K. Chan** and **V. Heine**, J. Phys. F 3, 795 (1973)

★ **G. Grüner**, Density Waves in Solids (Addison-Wesley, Reading, 1994) ★

1. Lets take one-dimensional electron gas...



2. Consider response of an electron gas to a time independent potential:

$$\phi(\vec{r}) = \int_{\vec{q}} \phi(\vec{q}) e^{i\vec{q}\vec{r}} d\vec{q}$$

3. Rearrangement of the charge density:

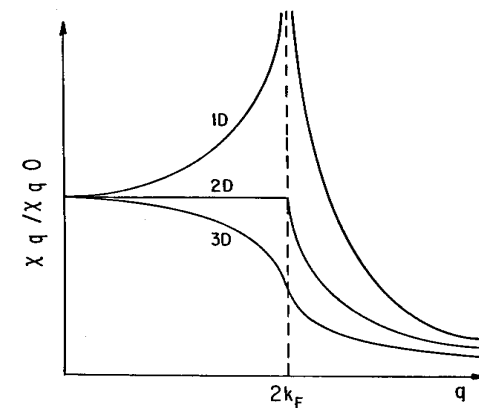
$$\rho^{ind}(\vec{q}) = \chi(\vec{q}) \phi(\vec{q})$$

4.  $\chi(q)$ —Lindhard response function:

$$\chi(\vec{q}) = \int \frac{d\vec{k}}{(2\pi)^d} \frac{f_{\vec{k}} - f_{\vec{k}+\vec{q}}}{\varepsilon_{\vec{k}} - \varepsilon_{\vec{k}+\vec{q}}}$$

In one dimension:

$$\chi(q) = \frac{-e^2}{\pi \hbar v_F} \ln \left| \frac{q + 2k_F}{q - 2k_F} \right|$$



$\chi(q)$  diverges at  $q=2k_F$

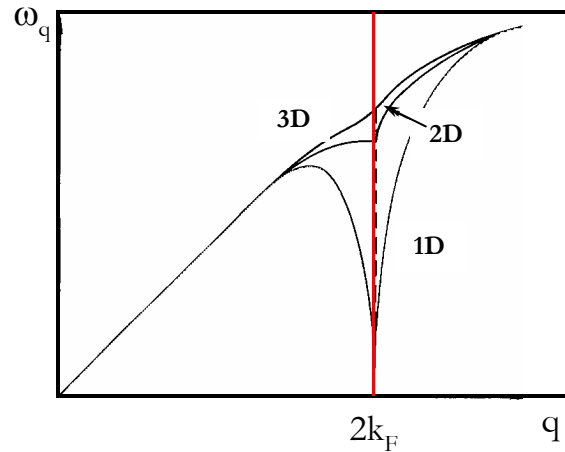


One-dimensional gas is unstable  
 with respect to the formation of a  
 periodically varying electron charge density

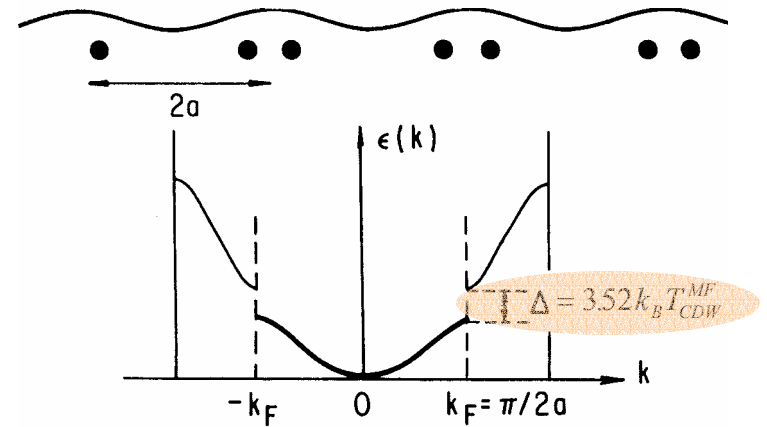
# Consequences of charge modulation

/and electron-phonon coupling/

Modification of phonon spectrum  
/Kohn anomaly or phonon softening at  $2k_F$ /

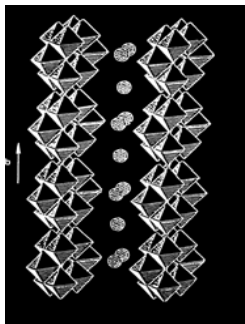


Periodic lattice modulation  
and Piers transition /opening of a gap at  $k_F$ /

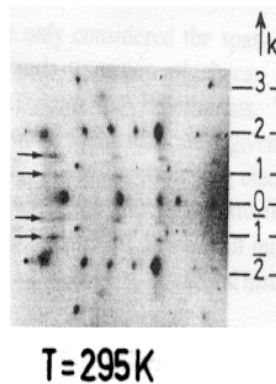


CDW in a real system:  $K_{0.3}MoO_4$

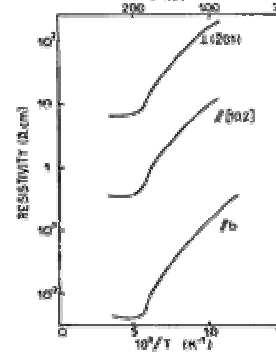
Quasi-one-dimensional  
crystal structure



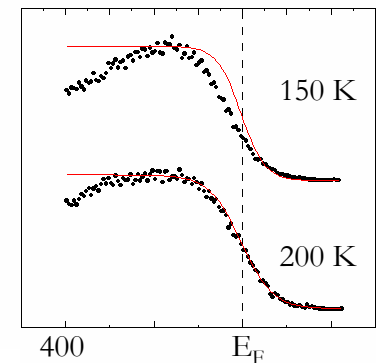
X-ray scattering



Resistivity



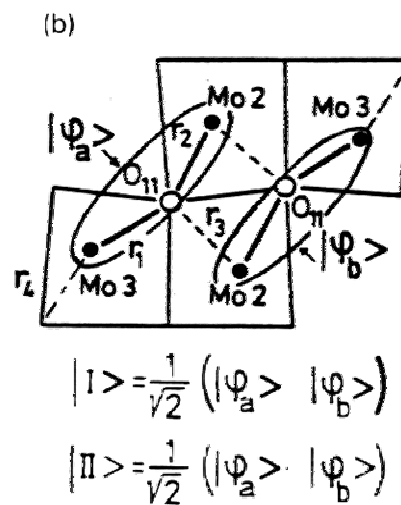
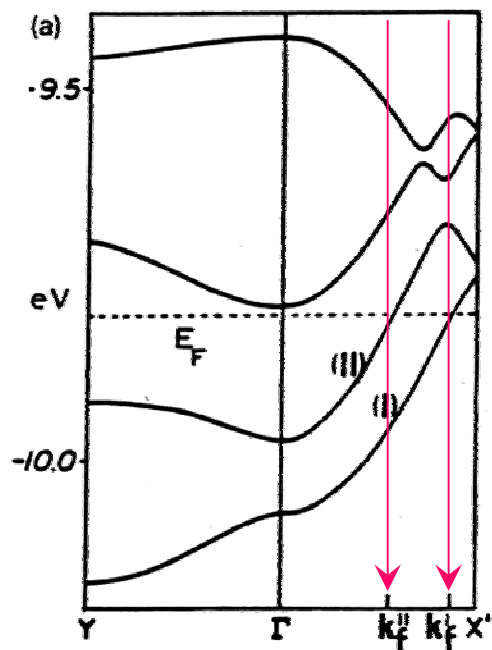
ARPES spectra at  $k_F$





# Electronic structure of $\text{K}_{0.3}\text{MoO}_3$ /tight-binding calculations/

*M.-H. Whangbo and L.F. Schneemeyer, Inor. Chem. 25,2424 (1986)*

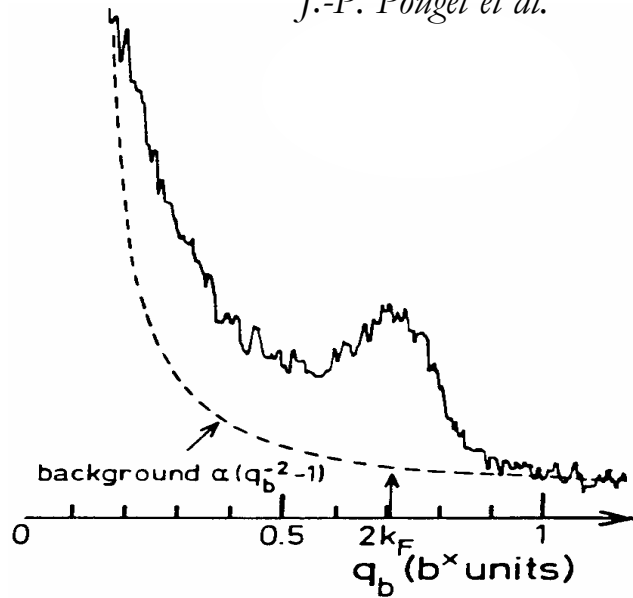


# Structural studies of CDW in $\text{K}_{0.3}\text{MoO}_3$

/incommensurate to commensurate transition/

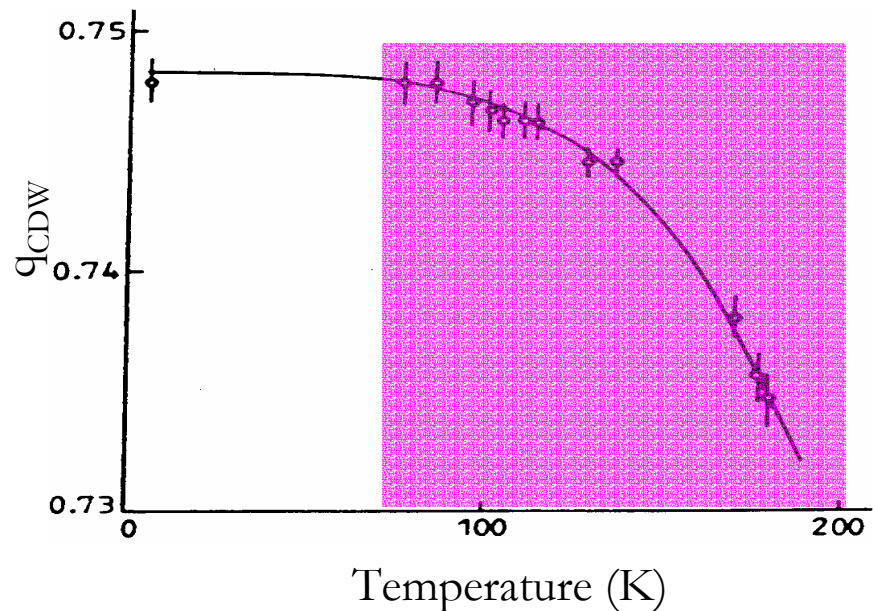
## Diffuse X-ray scattering

*J.-P. Pouget et al.*



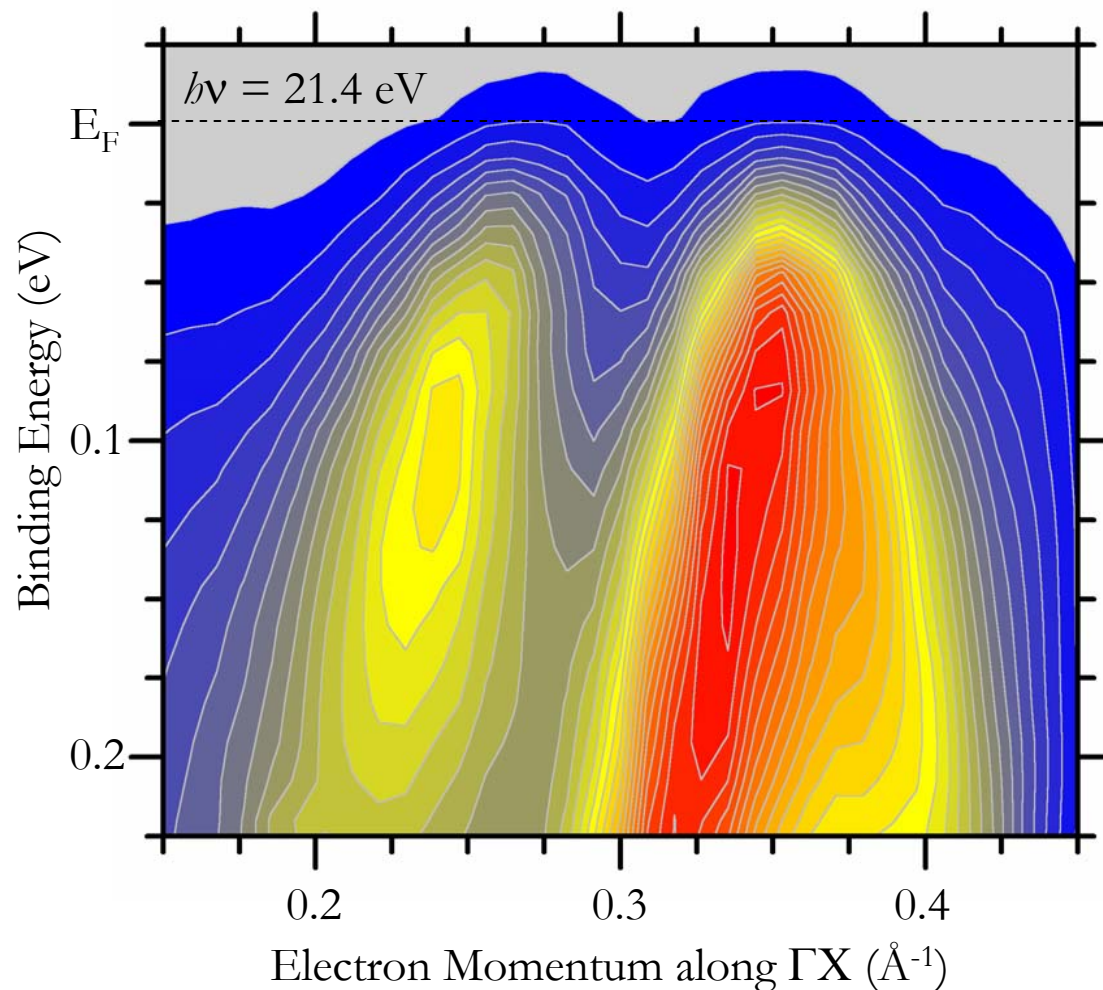
## Temperature dependent neutron scattering

*M.Sato, H. Fujishita and S.Hoshito,  
J. Phys. C: Solid State phys., 16, L877 (1983)*



# Direct monitoring electron bands in $\text{K}_{0.3}\text{MoO}_3$

/3-D maps of photocurrent/



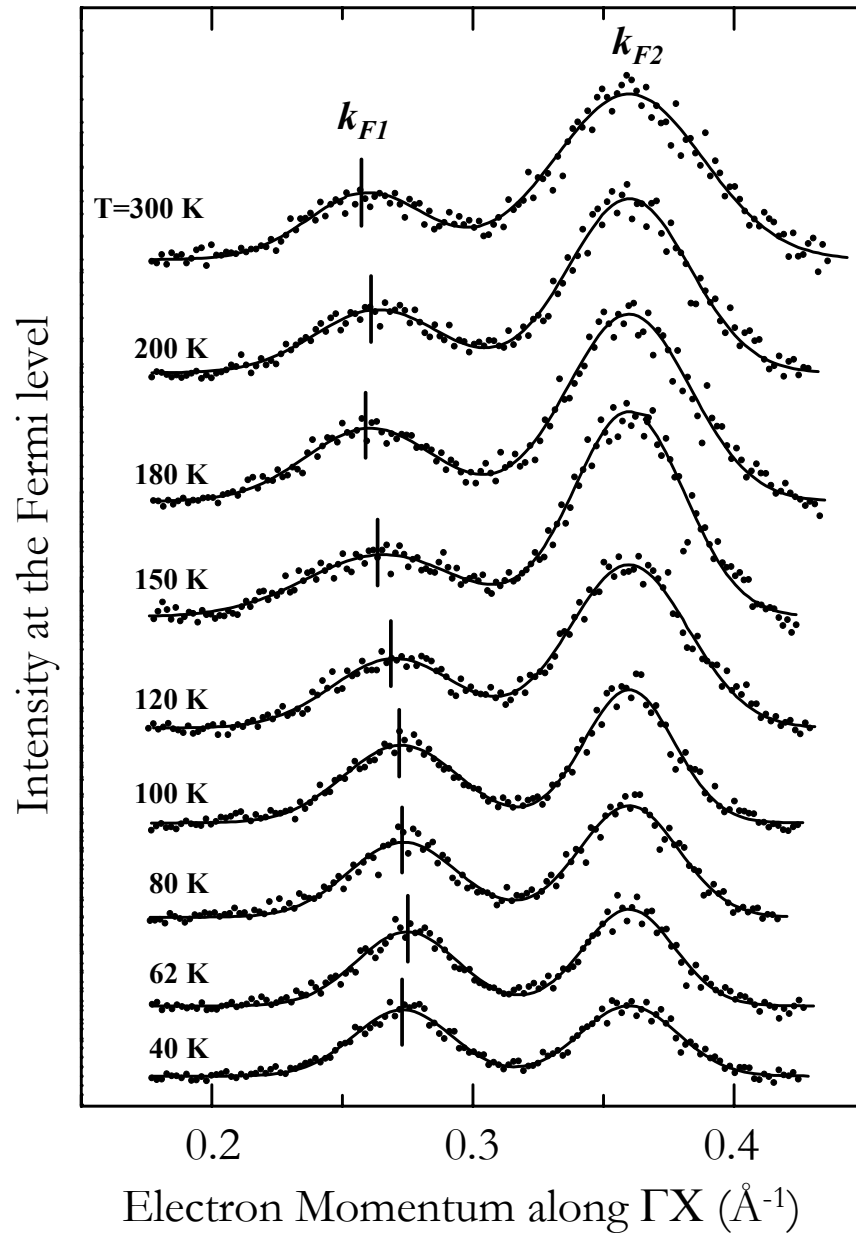
## Experimental details:

Samples cleaved *in situ*

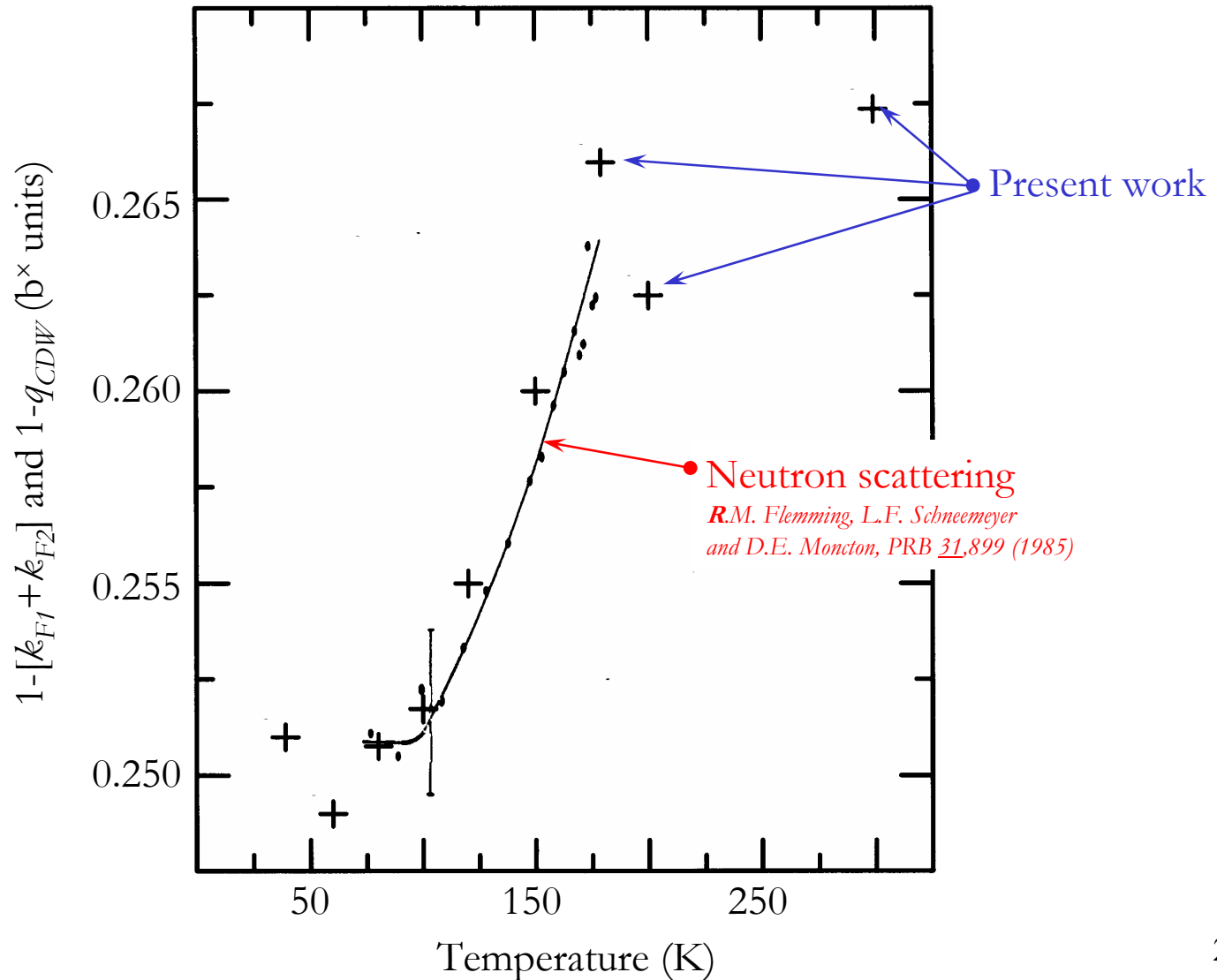
Liquid He cryostat provides  
temperatures from  
 $\sim 20 \text{ K}$  to  $\sim 450 \text{ K}$

Temperature monitored with  
OMEGA CY7 sensor

# Momentum Distribution Curves at $E_F$

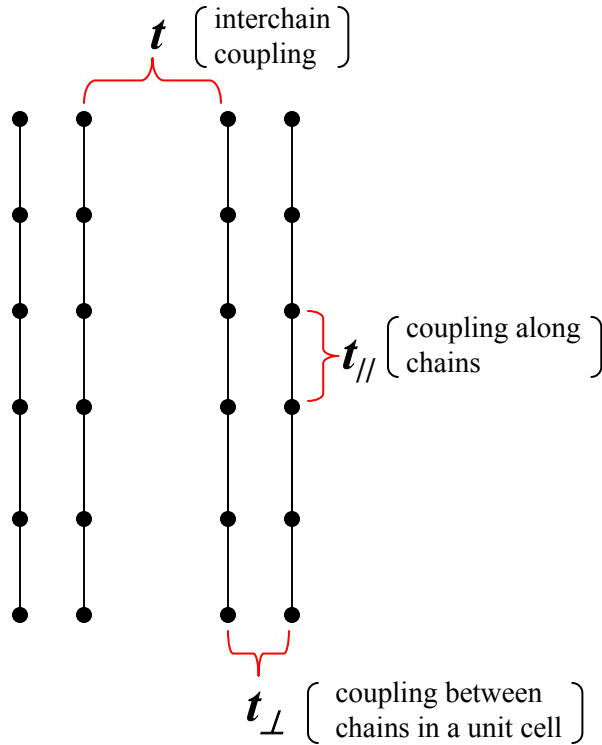


Incommensurate to commensurate CDW  
transition in  $\text{K}_{0.3}\text{MoO}_3$   
/viewed by photoemission/



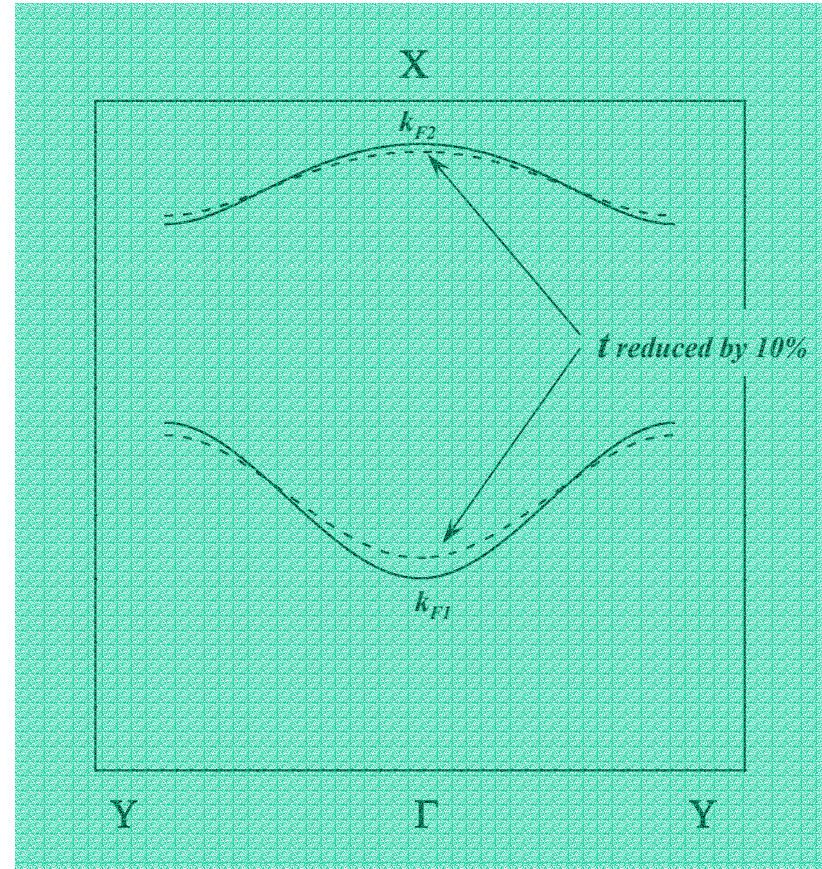
# Fermi surface of an array of coupled chains

/tight binding calculation/



Fermi surface is given by:

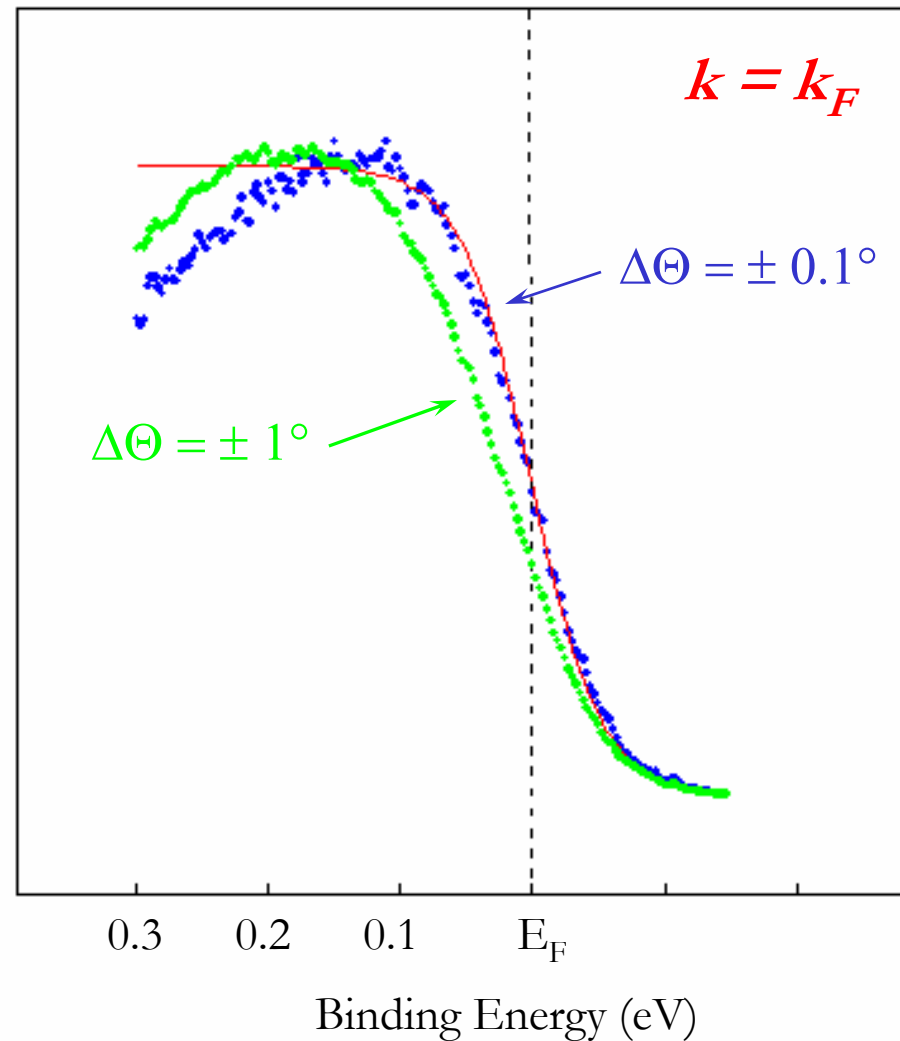
$$\mu = -2\cos(k_{//}) \pm (t_{\perp} + 2t_{\perp} t \cos(k_{\perp}) + t)^{1/2}$$



*A.V. Fedorov et al., Journal of Physics: Condensed Matter (Letters to the Editor) 12, L191 (2000)*



Suppression of spectral weight in photoemission  
from low-dimensional conductors:  
influence of momentum resolution



# Physical Review Letters

Home Page	Browse Available Volumes	Search	Subscriptions	Online Journal Help
Phys. Rev. Lett.	Vol	Page or Article #:	Retrieve	

Search Volumes 80 - Present: Results List

[New Search](#) [General Search Help](#)

Article Collection: [View](#) [Collect](#) [Help](#) (Click on ☐ to add an article.)

You were searching for : ((photoemission) <and>(brookhaven <IN> aff))  
 You found 10 out of 12056 (10 returned)  
 Documents 1 - 10 listed on this page

	Score	Title	Author(s)	Citation
<input checked="" type="checkbox"/>	79%	1 Doping and Temperature Dependence of the Mass Enhancement Observed in the Cuprate Bi[sub 2]S[ub 2]O[sub 8 + delta ]	Mass Johnson, T Valla, A V Fedorov, P D Johnson	Phys. Rev. Lett. 87, 177007 (2001)
<input checked="" type="checkbox"/>	79%	2 Many-Body Effects in Angle-Resolved Photoemission: Quasiparticle Energy and Lifetime of a Molecular Surface State	Johnson, T Valla, A V Fedorov, P D Johnson	Phys. Rev. Lett. 83, 2085 (1999)
<input checked="" type="checkbox"/>	79%	3 Temperature Dependent Photoemission Studies of Optimally Doped Bi[sub 2]S[ub 2]O[sub 8 + delta ]	Johnson, T Valla, A V Fedorov, P D Johnson	Phys. Rev. Lett. 82, 2179 (1999)
<input type="checkbox"/>	77%	4 Evidence of Electron Fractionalization from Photoemission Spectra in the High Temperature Superconductors	Orgad, S A Kivelson, E W Carlson	Phys. Rev. Lett. 86, 4362 (2001)
<input checked="" type="checkbox"/>	77%	5 Charge-Density-Wave-Induced Modification of Quasiparticle Self-Energy in 2H-TaSe[sub 2]	Johnson, T Valla, A V Fedorov, P D Johnson	Phys. Rev. Lett. 85, 4759 (2000)
<input checked="" type="checkbox"/>	77%	6 Reply: Smith et al.	Kevin E Smith, Xue, L-C Duda	Phys. Rev. Lett. 85, 3986 (2000)
<input checked="" type="checkbox"/>	77%	7 Temperature Dependent Scattering Rates at the Fermi Surface of Optimally Doped Bi[sub 2]S[ub 2]O[sub 8 + delta ]	Johnson, T Valla, A V Fedorov, P D Johnson	Phys. Rev. Lett. 85, 828 (2000)
<input checked="" type="checkbox"/>	77%	8 Electronic Structure near the Fermi Surface in the Quasi-One-Dimensional Conductor Li[sub 0.9]Mo[sub 0.1]O[sub 2]	Johnson, T Valla, A V Fedorov, P D Johnson	Phys. Rev. Lett. 85, 1235 (1999)
<input type="checkbox"/>	77%	9 Magnetic Properties at Surface Boundary of a Half-Metallic Ferromagnet La[sub 0.7]Sr[sub 0.3]O[sub 2]	Kim, H J Park, E Vesco	Phys. Rev. Lett. 81, 1953 (1998)

# Physical Review Letters

Home Page	Browse Available Volumes	Search	Subscriptions	Online Journal Help
Phys. Rev. Lett.	Vol	Page or Article #:	Retrieve	

Search Volumes 80 - Present: Results List

[New Search](#) [General Search Help](#)

Article Collection: [View](#) [Collect](#) [Help](#) (Click on ☐ to add an article.)

You were searching for : ((photoemission) <and>(shen <IN> author))  
 You found 12 out of 12056 (12 returned)  
 Documents 1 - 12 listed on this page

	Score	Title	Author(s)	Citation
<input checked="" type="checkbox"/>	79%	1 Anomalous Electronic Structure and Pseudogap Effects in Nd[sub 1.85]Ce[sub 0.15]CuO[sub 4]	N P Armitage, D Lu, C Kim	Phys. Rev. Lett. 87, 147003 (2001)
<input checked="" type="checkbox"/>	79%	2 Bilayer Splitting in the Electronic Structure of Heavily Overdoped Bi[sub 2]S[ub 2]O[sub 8 + delta ]	D L Feng, N P Armitage, D H Lu	Phys. Rev. Lett. 86, 5550 (2001)
<input checked="" type="checkbox"/>	79%	3 Superconducting Gap and Strong In-Plane Anisotropy in Untwinned YBa[sub 2]Cu[sub 3]O[sub 7 - delta ]	D H Lu, D L Feng, N P Armitage	Phys. Rev. Lett. 86, 4370 (2001)
<input checked="" type="checkbox"/>	79%	4 Superconducting Gap Anisotropy in Nd[sub 1.85]Ce[sub 0.15]CuO[sub 4]: Results from Photoemission Spectroscopy	N P Armitage, D Lu, D L Feng	Phys. Rev. Lett. 86, 1126 (2001)
<input checked="" type="checkbox"/>	79%	5 Fermi Surface, Surface States, and Surface Reconstruction in Sr[sub 2]RuO[sub 4]	A Damascelli, D Lu, K M Shen	Phys. Rev. Lett. 85, 5194 (2000)
<input checked="" type="checkbox"/>	77%	6 Dual Nature of the Electronic Structure of (La[sub 2 - x]Nd[sub x]Sr[sub 1]CuO[sub 4]) and La[sub 2]CuO[sub 4]	Yoshida, S A Kivelson	Phys. Rev. Lett. 86, 5578 (2001)
<input type="checkbox"/>	77%	7 Evidence of Electron Fractionalization from Photoemission Spectra in the High Temperature Superconductors	Kivelson, E W Carlson	Phys. Rev. Lett. 86, 4362 (2001)
<input checked="" type="checkbox"/>	77%	8 Angle-Resolved Photoemission Study of Insulating and Metallic Cu-O Chains in PrBa[sub 2]Cu[sub 3]O[sub 7 - delta ]	D H Lu, C Kim, Z-X Shen	Phys. Rev. Lett. 85, 4779 (2000)
<input checked="" type="checkbox"/>	77%	9 Evidence for an Energy Scale for Quasiparticle Dispersion in Bi[sub 2]S[ub 2]O[sub 8 + delta ]	P V Bogdanov, A Lanzara, S A Kivelson	Phys. Rev. Lett. 86, 2581 (2001)